KfK 4453
Oktober 1988

Extended Sum-Rule Model for Intermediate Mass-Fragment Emission

I. M. Brâncuş
Institut für Kernphysik

Kernforschungszentrum Karlsruhe

KERNFORSCHUNGSZENTRUM KARLSRUHE

Institut für Kernphysik

KfK 4453

EXTENDED SUM-RULE MODEL FOR INTERMEDIATE MASS-FRAGMENT EMISSION

I.M. Brâncuş*

*Permanent address: Central Institute of Physics, IPNE
Bucharest (Romania)

Kernforschungszentrum Karlsruhe GmbH, Karlsruhe

Kernforschungszentrum Karlsruhe GmbH
Postfach 3640, 7500 Karlsruhe 1

ISSN 0303-4003

EXTENDED SUM-RULE MODEL FOR
INTERMEDIATE MASS-FRAGMENT EMISSION

A survey is given on the basis of sum-rule models describing the intermediate mass-fragment emission in light and heavy ion reactions. The original sum -rule worked out by Wilczyński et al. has been extended by a term accounting for the dynamical behaviour of the dinuclear system and dependent on the critical value of the orbital angular momentum for the fusion with dissipation. This term proves to be rather essential in reproducing the Z-distribution of the fragments emitted from rather asymmetric systems. The features of the model are demonstrated by applying it to ^{40}Ar + ^{nat}Ag, ^{40}Ar + ^{154}Sm, ^{40}Ar + ^{197}Au, ^{40}Ar + ^{232}Th (E = 336 MeV), and to ^{6}Li + ^{46}Ti, ^{6}Li + ^{nat}Cu, ^{6}Li + ^{nat}Ag (E = 156 MeV) reactions.

EIN ERWEITERTES SUMMENREGEL-MODELL ZUR BESCHREIBUNG
DER EMISSION VON NUKLEAREN FRAGMENTEN MITTLERER MASSE

Es wird ein Überblick gegeben über die Grundlagen von Summenregel-Modellen zur Beschreibung der Emission von nuklearen Fragmenten mittlerer Masse bei Leicht- und Schwerionenreaktionen. Das ursprüngliche Modell von Wilczyński et al. wird erweitert mit einem Term, der das dynamische Verhalten des kurzlebigen dinuklearen Systems in Rechnung stellt und abhängig ist vom kritischen Bahndrehimpuls für eine Fusion unter Dissipation. Dieser Term erweist sich als wichtig, um die Z-Verteilungen der Fragmente aus einem asymmetrischen System zu beschreiben. Die Charakteristika des Modells werden demonstriert mit einer Anwendung auf ^{40}Ar + ^{nat}Ag ^{40}Ar + ^{nat}Ag, ^{40}Ar + ^{154}Sm, ^{40}Ar + ^{197}Au, ^{40}Ar + ^{232}Th (E = 336 MeV), und auf ^{6}Li + ^{46}Ti, ^{6}Li + ^{nat}Cu, ^{6}Li + ^{nat}Ag (E = 156 MeV) Reaktionen.

1. Introduction

The study of heavy ion collisions has revealed interesting features of the reaction mechanism of complex nuclear particles. Above the Coulomb barriers, fusion and incomplete fusion processes, deep inelastic collisions and the emission of intermediate mass fragments have been shown to exhibit features which can be understood neither from a point of view of a direct process nor by assuming the formation of a completely equilibrated compound nucleus. Obvious characteristics are:

- a large number of nucleons is transferred between the reaction partners.
- the angular distribution show a peak at the grazing angle, which is characteristic for a fast process.
- the cross section depends nearly linearly on the groundstate Q_{gg} - value which has been shown to be a feature of a statistical reaction mechanism.

New ideas have been developped to explain these new features. One of the most important concepts introduced to describe the underlying reaction mechanisms is the concept *partial statistical equilibrium*, i.e. the assumption that the system of colliding ions approaches a statistical equilibrium with respect to a subset of the degrees of freedom. This concept resulted from the understanding of a large variety of multinucleon transfer reactions /1/.

In a statistical reaction the cross section is proportional to the level density of the system, which can be given by a constant temperature formula:

$$\rho(U) = \frac{1}{T_0} \, exp\left(\frac{U}{T_0}\right) \qquad (1)$$

where the temperature T_0 is adjusted empirically. The excitation energy is given by:

$$U = Q_{gg} - Q_c - Q_{ex} - P(Z) - P(N) \qquad (2)$$

where Q_{gg} is the Q-value of the ground state, Q_c is the change of Coulomb interaction energy due to charge transfer, Q_{ex} represents the other excitation processes (identical for all exit channels), and P(N) and P(Z) are pairing corrections

A further important concept introduced into fusion models is the *critical angular momentum* /2/. Assuming that the two nuclei can be considered as two spherical liquid drops, the critical angular momentum for fusion can be derived from the condition that the nuclear, Coulomb and centrifugal forces are in balance.

When increasing the incident energies, incomplete fusion reactions have been observed and the *concept of critical angular momentum* has been generalized and invoked to explain the incomplete fusion in $^{12}C + {}^{169}Gd$ collisions /3/. The assumption was made that the angular momentum limitation in the entrance channel governs the competition between complete and incomplete fusion, and that the heavier fragment is preferentially captured. Each fragment of the projectile carries away a part of the angular momentum which is proportional to its mass.

2. The sum-rule model

Using the two basic concepts of the partial statistical equilibrium and the critical angular momentum, the *sum-rule-model* for fusion and incomplete fusion processes has been elaborated by J. Wilczyński et al. /4,5/. Thereby the reaction probability for each reaction channel (i) proceeding via a partial statistical equilibrium is taken proportional to the exponential factor proposed by Bondorf et al. /1/:

$$P(i) \propto exp\ \{ [\ Q_{gg}(i) - Q_c\ (i)\ ] / T \} \qquad (3)$$

where T is the effective temperature, Q_c is the change of the Coulomb interaction energy due to the transfer of charge:

$$Q_c = (Z_1^f Z_2^f - Z_1^i Z_2^i)\, e^2 / R_c \qquad (4)$$

Z_1^i, Z_2^i and Z_1^f, Z_2^f are the atomic numbers of the constituents of the dinuclear system before and after the transfer of charge. The quantity R_c is an effective relative distance where the transfer of charge takes place.

In addition, it is postulated that any transfer of mass may occur if the angular momentum of the relative motion of the captured fragment (n or m) with respect to the absorbing nucleus (A_2 or A_1) is smaller than the limiting angular momentum for this system:

$$\ell\,(\text{n vs } A_2 \text{ or m vs } A_1) \leqq \ell_{\ell im}\,(\text{n vs } A_2 \text{ or m vs } A_1). \qquad (5)$$

The limiting angular momentum is related to the critical angular momentum:

$$l_{lim}\,(A_1\ vs\ A_2) = \frac{A_1 A_2}{mA_1 + nA_2}\, l_{cr}\,(n\ vs\ A_2\ or\ m\ vs\ A_1) \qquad (6)$$

where ℓ_{cr} is calculated with the condition that a given fragment can be captured only if it penetrates into the region of attraction in the nucleus-fragment potential, thus using the relation:

$$\left(l_{cr} + \frac{1}{2}\right)^2 = \mu \frac{(C_1 + C_2)^3}{\hbar^2} \left[4\pi\gamma \frac{C_1 C_2}{C_1 + C_2} - \frac{Z_1 Z_2 e^2}{(C_1 + C_2)^2} \right] \tag{7}$$

where C_1, C_2, are the half-density radii of the interacting nuclei A_1, A_2 and γ is the surface energy coefficient (see refs. 4,5).

A smooth cut-off in the ℓ-space for each individual reaction channel (i) it is introduced by parametrizing the transmission coefficients as:

$$T_{l(i)} = \left\{ 1 + exp \left[\frac{l - l_{lim(i)}}{\Delta l} \right] \right\}^{-1} \tag{8}$$

with $\Delta\ell$ being a parameter describing the "diffuseness" of the T_ℓ distributions in the ℓ-space.

The cross sections for each reaction channel are given without any further adjustable factor by the expression:

$$\sigma(i) = \pi \lambda^2 \sum_{l=o}^{l_{max}} (2l+1) \frac{T_{l(i)} P(i)}{\sum_j T_{l(j)} P(j)} \tag{9}$$

based on the following sum-rule for the reaction probabilities:

$$N_l \sum_i T_{l(i)} P(i) = 1 \tag{10}$$

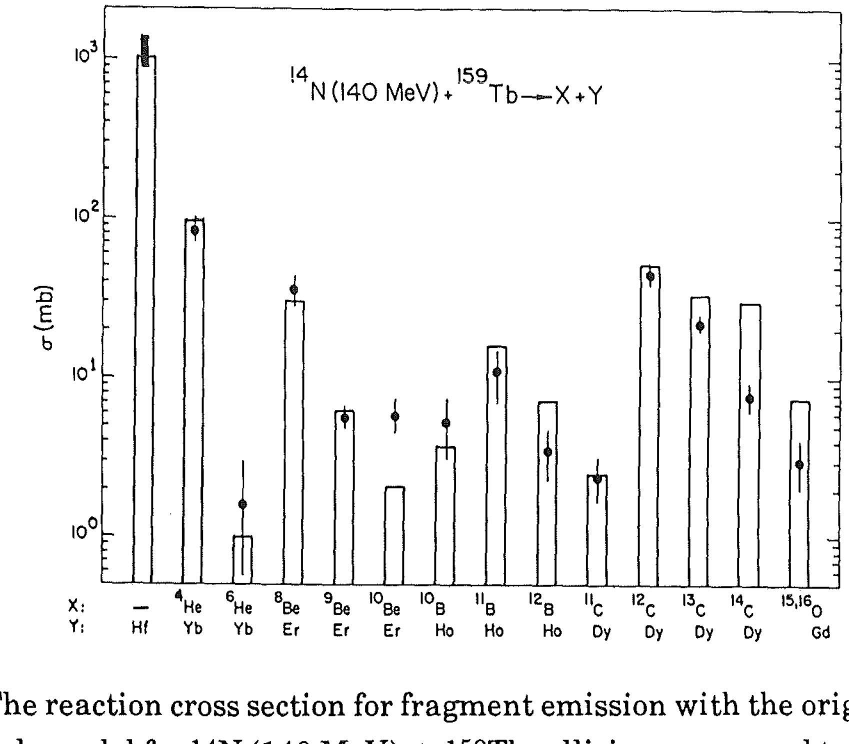

Fig. 1 The reaction cross section for fragment emission with the original sum-rule model for ^{14}N (140 MeV) + ^{159}Tb collisions compared to experimental results from ref. 5.

The numbers N_ℓ are normalization factors common for all reaction channels. The limit ℓ_{max} value is defined as the largest ℓ for which the colliding system penetrates into a region when the total nucleus-nucleus potential is attractive.

The model implies three parameters: T, R_c and $\Delta\ell$, which are usually determined from the best fit to the experimental cross sections.

In fig. 1 the predictions of the sum-rule model are compared to experimental cross sections for the ^{14}N (140 MeV) + ^{159}Tb reactions /5/.

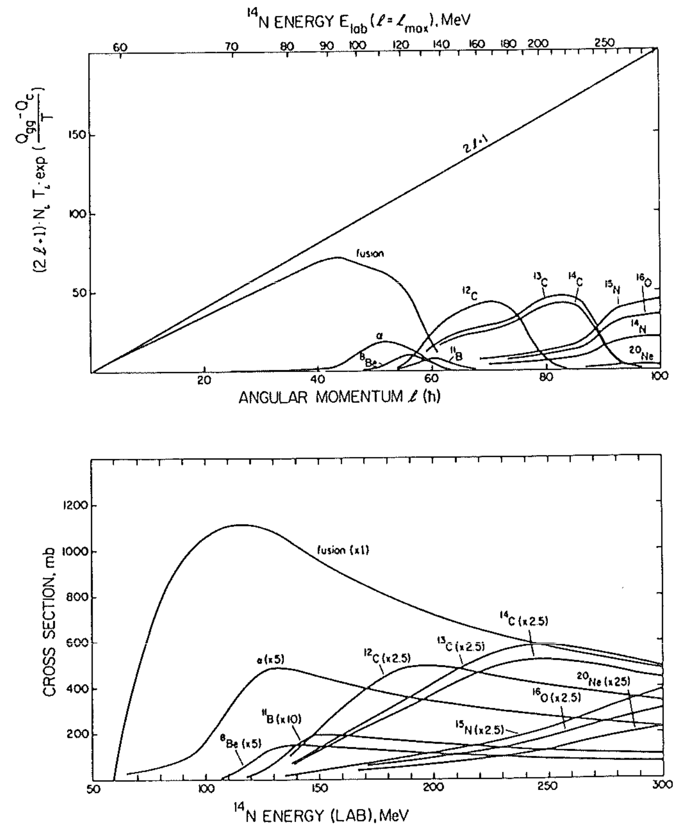

Fig. 2 The partial cross sections σ_ℓ calculated with the original sum-rule model for the ^{14}N (140MeV) + ^{159} Tb reactions (from ref. 5)

In fig. 2 the ℓ-dependence of the cross sections for different reaction channels in ^{14}N + ^{159}Tb reaction is presented /5/. It can be seen that the sum-rule model predicts a very specific localization of various reaction channels in the ℓ-space.

3. Intermediate mass fragment emission

In recent years intermediate mass-fragment emission has been definitively observed in heavy ion collisions, opening questions about the origin of such reaction products. While for relatively low bombarding energies the phenomena seem to originate from equilibrated sources at relatively low excitation energies, both equilibrium and non-equilibrium mechanisms might coexist at intermediate energies.

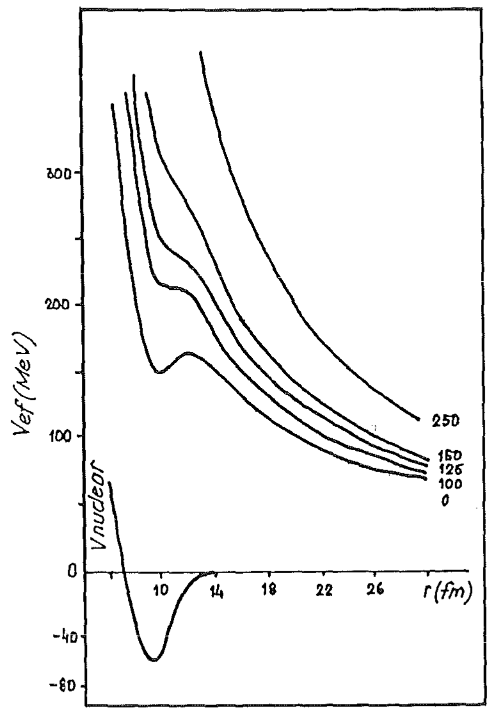

Fig. 3

The interaction potential for the $^{40}Ar + ^{197}Au$ system for different angular momenta /12/.

Recently a new mechanism called centrifugal fragmentation was proposed by V.V. Volkov /6/ to explain the emission of long-lived intermediate mass reaction products. This approach is based on the assumptions that both in complete fusion and in the deep inelastic reactions, the same conservative (nuclear, Coulomb and centrifugal) forces are acting. Also in both processes, the dissipation forces are due to nuclear friction. The yields of the reaction products from complete fusion and from deep inelastic transfers obey the Q_{gg} systematics /7/. The deep inelastic reactions take place for angular momenta higher than the critical value for fusion. On its way towards fusion, the dinuclear system can desintegrate due to mass transfer and to increased centrifugal forces.

4. Fusion dynamics in heavy ion collisions

It has been pointed out by C. Ngô/8/ that the dissipation plays an important role in fusion processes of heavy ions. The simplest dynamical model to describe the collision of two heavy ions implies two macroscopic degrees of freedom: The distance between the center-of-mass of two nuclei and the deflection angle /9/. Using a proximity nuclear potential /10/ and assuming that the dissipation is due to frictional forces /11/ the classical trajectories have been calculated for the ^{90}Ar (300 MeV) + ^{197}Au system /12/. In fig. 3 the interaction potential is plotted as a sum of nuclear and Coulomb potential. In fig. 4 the classical trajectories for deeply inelastic collisions in the ^{40}Ar (300 MeV) + ^{197}Au systems are shown for different angular momenta. It results that for ℓ values less than the critical value ℓ_{cr} = 125 the dissipation is so large so that fusion takes place.

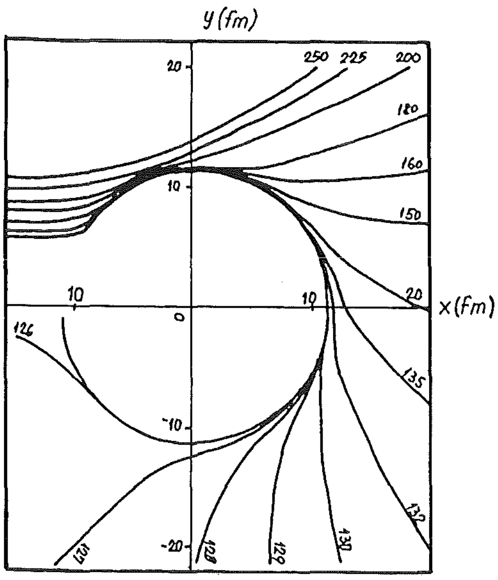

Fig. 4

Classical trajectories calculated for different angular momenta in the ^{40}Ar + ^{197}Au system at 300 MeV /12/.

In the dynamical model developed by T. Suomijarvi et al. /13/ the equations of motion are the following:

$$\mu \frac{d^2R}{dt^2} = \frac{\partial V_l(R)}{\partial R} - C_R\, g(R)\, \dot{R} \tag{11}$$

$$\frac{dl}{dt} = - \frac{C_t}{\mu} g(R) \; (l - l_{st}) \tag{12}$$

Here C_R g(R) and C_t g(R) are the radial and tangential friction forces. The orbital angular momentum is required to be larger than the sticking value ℓ_{st} which is the limiting case when the two nuclei stick to each other.

Using $C_R = 2C_t = 31{,}000$ MeV fm^{-2} (10^{-23} s)^2 for the radial friction coefficient, a good agreement between the calculated and the experimental fusion cross sections was observed for various different systems /8/.

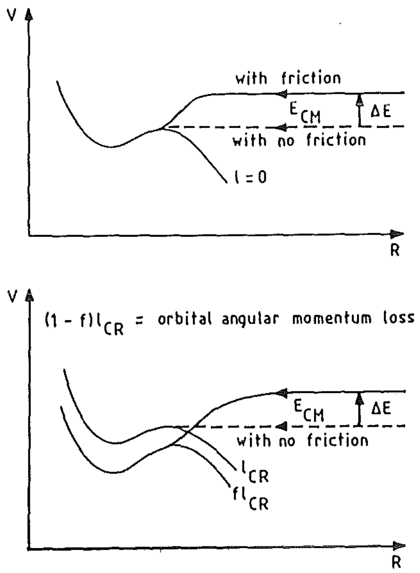

Fig. 5 Illustration of the effective interaction potential in cases with and without friction, of the dynamical energy surplus ΔE and of the orbital angular momentum loss /8/.

In such a dynamical picture, sketched in fig. 5, for both head-on and noncentral collisions, an additional amount of kinetic energy ΔE, called *dynamical energy surplus*, is necessary to compensate the friction acting in the system before it reaches the static fusion barrier. As emphasized by Ngô /8/ the dynamical fusion barrier is a sum of the static fusion barrier (as for the non dissipative case) and of the dynamical energy surplus.

Only at low incident energy ΔE ~ 0 the dynamical fusion barrier is practically identical to the static one. In addition, there is also an angular momentum loss changing the critical value for fusion.

By solving the equations of motion for each ℓ-value, the case when the system is trapped and the critical ℓ-value for fusion process with dissipation can be determined.

5. Extended sum-rule model

With the view that the light products are emitted from the dinuclear system on its route to complete fusion, it appears natural to assume that the transmission coefficients depend on the critical ℓ-value for fusion calculated for a dissipative process..

Furthermore assuming that this mechanism also proceeds by a partial statistical equilibration, we propose the following extended sum-rule for a partial wave:

$$N_l \left\{ \sum_{i=1}^{n} T_{l(i)} P(i) + \sum_{i=2}^{n} T_l' \; P(i) \right\} = 1 \qquad . \tag{13}$$

Here N_ℓ is a common ℓ-dependent normalization factor which takes into account all contributions of binary processes: fusion, incomplete fusion and IMF emission from a dinuclear system. The relative weight P(i) represents the reaction probability for a given channel (i). Two forms are used for the transmission coefficients:

$$T_{l(i)} = \left\{ 1 + exp \left[(l - l_{lim}(i)) / \Delta l \right] \right\}^{-1} \tag{14}$$

$$T_l' = \left\{ 1 + exp \left[(l - l_{cr}^{dyn}) / \Delta l \right] \right\}^{-1} \tag{15}$$

It should be noticed that only the $T_{\ell(i)}$ coefficients depend on the angular momentum limitation of the entrance channel.

Tab. 1 The critical values for fusion and the dynamical energy surplus calculated for a dissipative process. Experimental values of ℓ_{cr} are quoted in ref. 8.

Reaction		ℓ_{cr}^{dyn}	ℓ_{cr}^{exp}	ΔE (MeV)
^{40}Ar (336MeV) +	^{nat}Ag	113	118	80
	^{154}Sm	133	137	70
	^{197}Au	135	143	63
	^{232}Th	137		56
^{6}Li (156 MeV) +	^{46}Ti	39		42
	^{nat}Cu	45		36
	^{nat}Ag	51		29

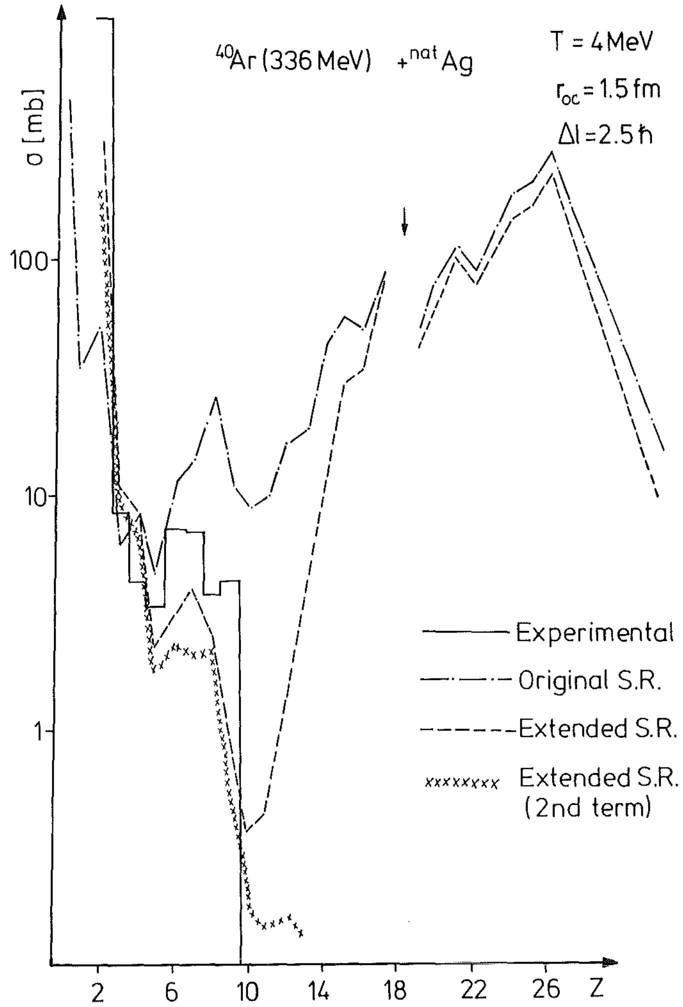

Fig. 6 Experimental and theoretical cross sections for the ^{40}Ar + ^{nat}Ag system at E = 336 MeV.

With eq. 13 the cross sections for each reaction channel (i) can be written as a sum of two contributions:

$$\sigma^{tot}(i) = \sigma(i) + \sigma'(i) \tag{16}$$

where

$$\sigma(i) = \pi\lambda^2 \sum_{l=0}^{l_{max}} (2l+1) \frac{T_{l(i)} P(i)}{\sum_{i=1}^{n} T_{l(i)} P(i) + \sum_{i=2}^{n} T_l' P(i)} \tag{17}$$

and

$$\sigma'(i) = \pi\lambda^2 \sum_{l=0}^{l_{max}} (2l+1) \frac{T_l' P(i)}{\sum_{i=1}^{n} T_{l(i)} P(i) + \sum_{i=2}^{n'} T_l' P(i)} \qquad (18)$$

The first part σ(i) represents the fusion (i = 1) and incomplete fusion processes (i ≧ 2) and σ '(i) describes the emission of light particles from a dinuclear system. It should be noticed that in eq. 13 the summation over the reaction channels starts with i = 2 in the second term. The model implies three parameters: T, R_c and $\Delta\ell$ like in the original version.

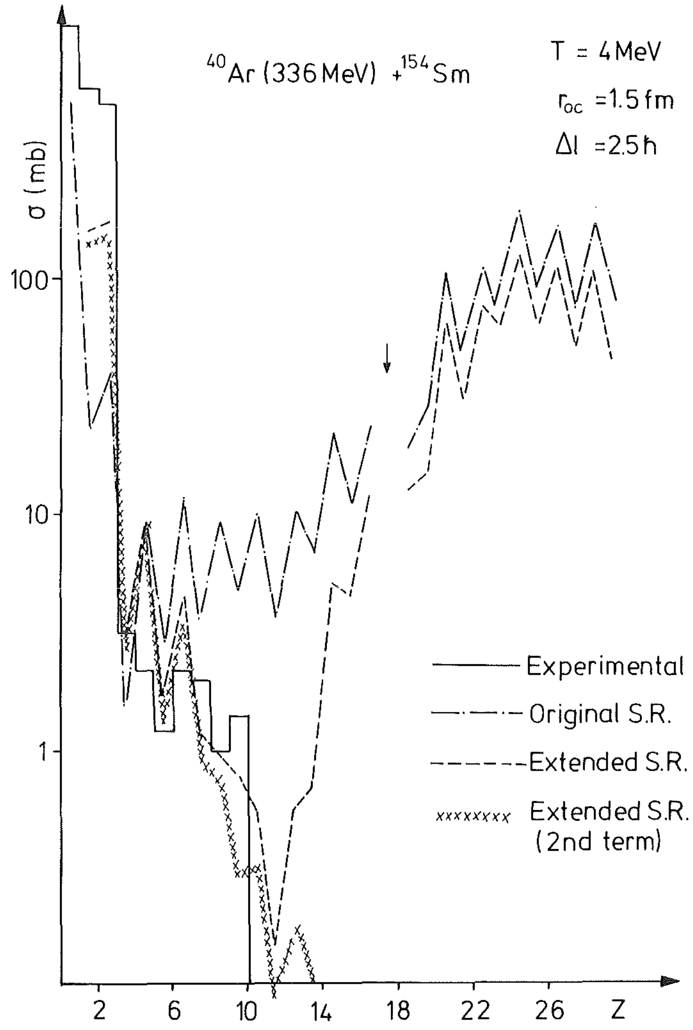

Fig. 7 Experimental and theoretical cross sections for the $^{40}Ar + {}^{154}Sm$ system at E = 336 MeV.

For demonstration and for further applications to specific cases tab. 1 presents the values of the critical angular momentum and the dynamical energy surplus resulting from calculations on the basis of a dynamical fusion model (sect. 4).

6. Analysis of large-angle emission for $3 \leqq Z \leqq 9$ products from collisions of 336 MeV ^{40}Ar ions with heavy targets.

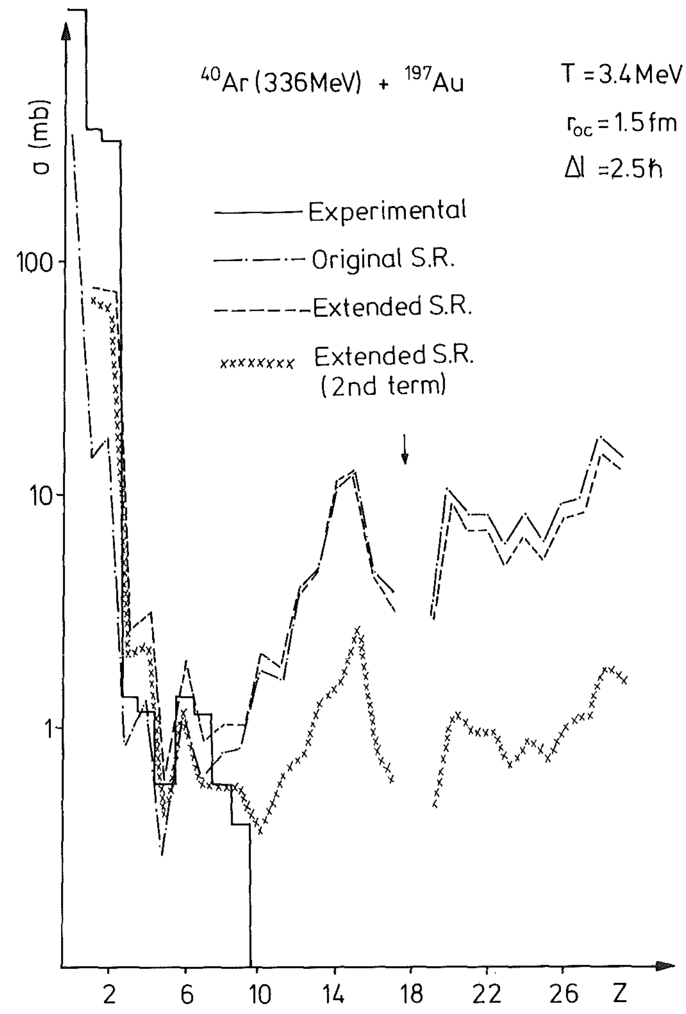

Fig. 8 Experimental and theoretical cross sections for the ^{40}Ar + ^{197}Au system at E = 336 MeV.

Measurements of intermediate mass-fragments ($3 \leqq Z \leqq 9$) from reactions of 336 MeV ^{40}Ar with ^{nat}Ag, ^{154}Sm, ^{197}Au /14/ and ^{232}Th /15/ have been reported and cross sections are available in literature.

Figs. 6 -8 compare the experimental data (histogramms) with the calculated (absolute) cross section values, as predicted by the original and extended sum-rule model. It may be noted that the extended version is able to predict the increased α-particle emission and the reduced production of elements with Z = 8, 9, thus improving the agreement with the experimental data.

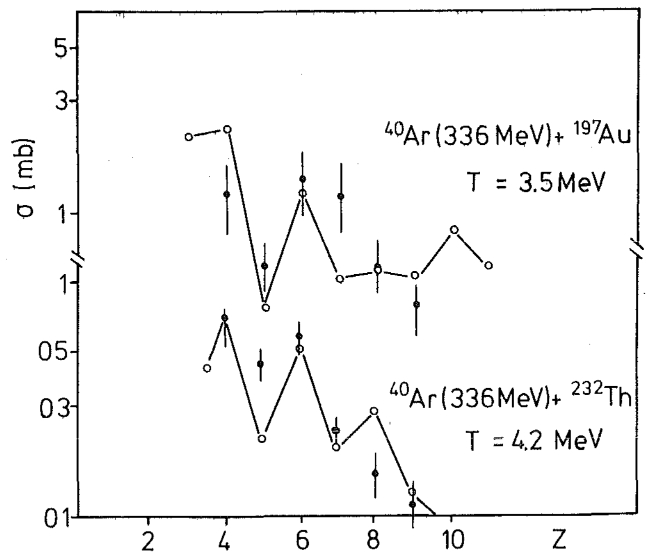

Fig. 9 The calculated cross sections σ' (eq. 19) and experimental data for 336 MeV ^{40}Ar colliding with ^{197}Au and ^{232}Th (R_c = 1,5 fm, $\Delta\ell$ = 2,5 $\hbar$).

Assuming that the large angle emission of $3 \leqq Z \leqq 9$ products originates from the dinuclear system on its way to complete fusion, the cross section (eq.18) for such long-lived products can be simply written as:

$$\sigma'(i) = \pi\lambda^2 \sum_{l=1}^{l_{cr}^{dyn}} \eta(l)\, P(i) \qquad (19)$$

with:

$$\eta(\ell) = (2\ell + 1) N_\ell T_\ell' \qquad (20)$$

Fig, 9 compares the calculated σ' (i) (eq. 19) with the experimental data for the ^{40}Ar + ^{197}Au and ^{232}Th cases. The good agreement observed implies that the mechanism for large-angle emission is governed by the Q_{gg}-systematics.

In figs. 10-11 the calculated partial cross sections are presented. We notice the variation in the localization in the ℓ-space for different incomplete fusion channels while the emission of the heavier products from a transient dinuclear system appears to be fairly well concentrated around the critical ℓ-values for fusion with dissipation.

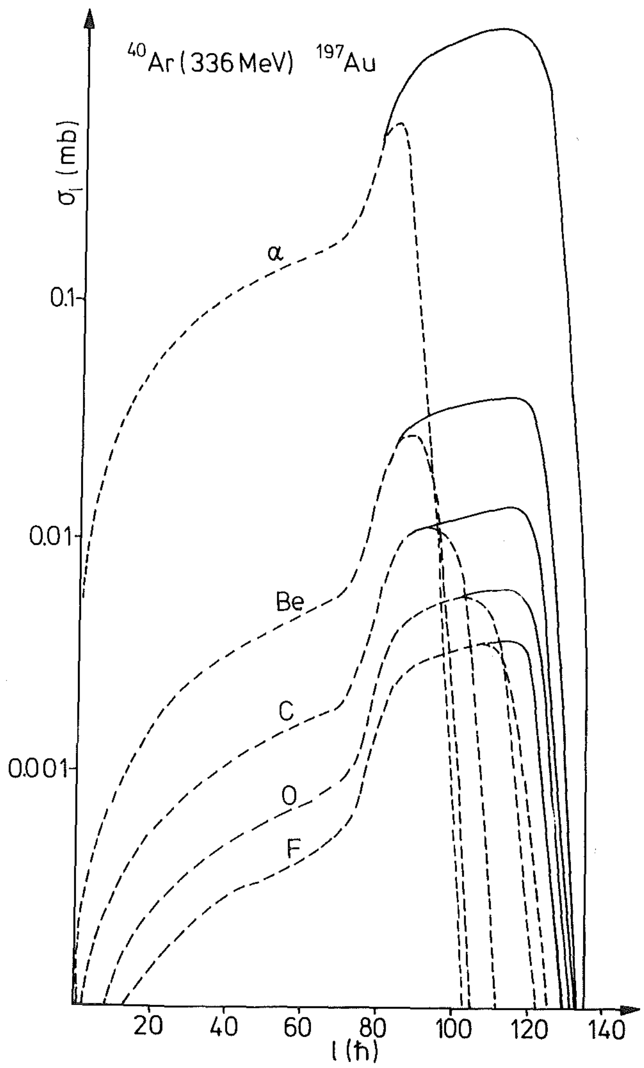

Fig. 10

The partial cross sections σ_ℓ calculated with the original and the extended version of the sum-rule model: ^{40}Ar + ^{197}Au at 336 MeV ($\ell_{cr}^{dyn} = 135\hbar$).

7. Analysis of IMF emission in ^{6}Li induced reactions at 156 MeV

Measurements of intermediate mass fragment emission from the rather asymmetric systems of 156 MeV ^{6}Li colliding with ^{46}Ti, ^{nat}Cu and ^{nat}Ag have been recently reported /16, 17/.

As evident from figs. 12-14 the original sum-rule model applied for such high incident energies leads to a considerable underestimation of the IMF emission, in particular for Cu and Ag targets. The discrepancies are largely removed by taking into account the second term of eq. 16 (figs. 15-17). The large improvement in predicting the IMF emission, especially for the heavier targets, is remarkable. In addition the predictions for alpha-particle emission are considerably improved, too. When fitting the experimental data (using the program IMFREM / 18 /), it has been found that the results are rather insensitive to $\Delta\ell$ which has been finally fixed to $3\hbar$. However, there appear considerable parameter correlations between T and R_c. Thus, the resulting values cannot be independently discussed.

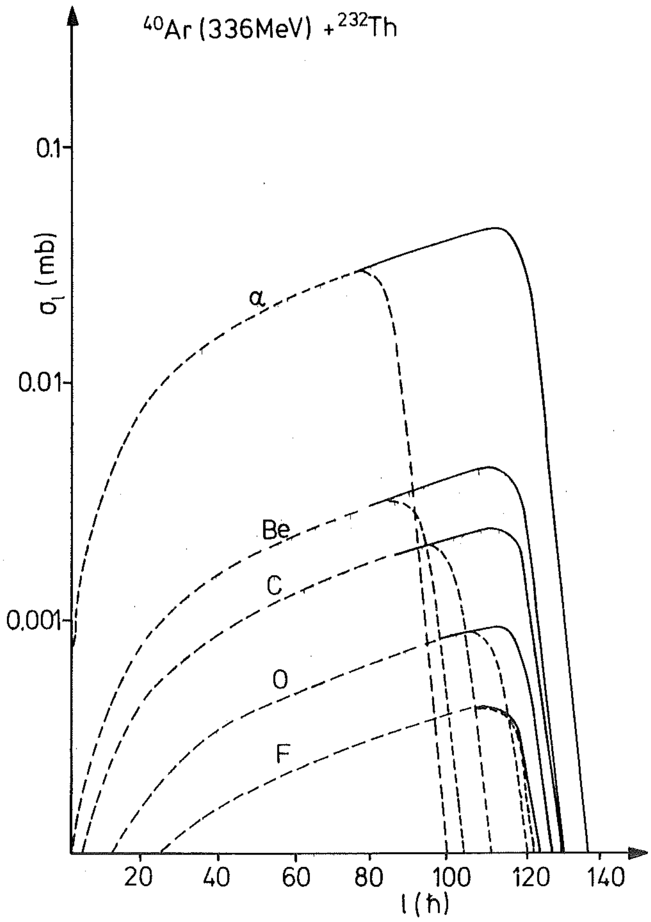

Fig. 11 The partial cross sections σ_ℓ calculated with the original and the extended version of the sum-rule model: ^{40}Ar + ^{232}Th at 336 MeV ($\ell_{cr}{}^{dyn} = 137\hbar$).

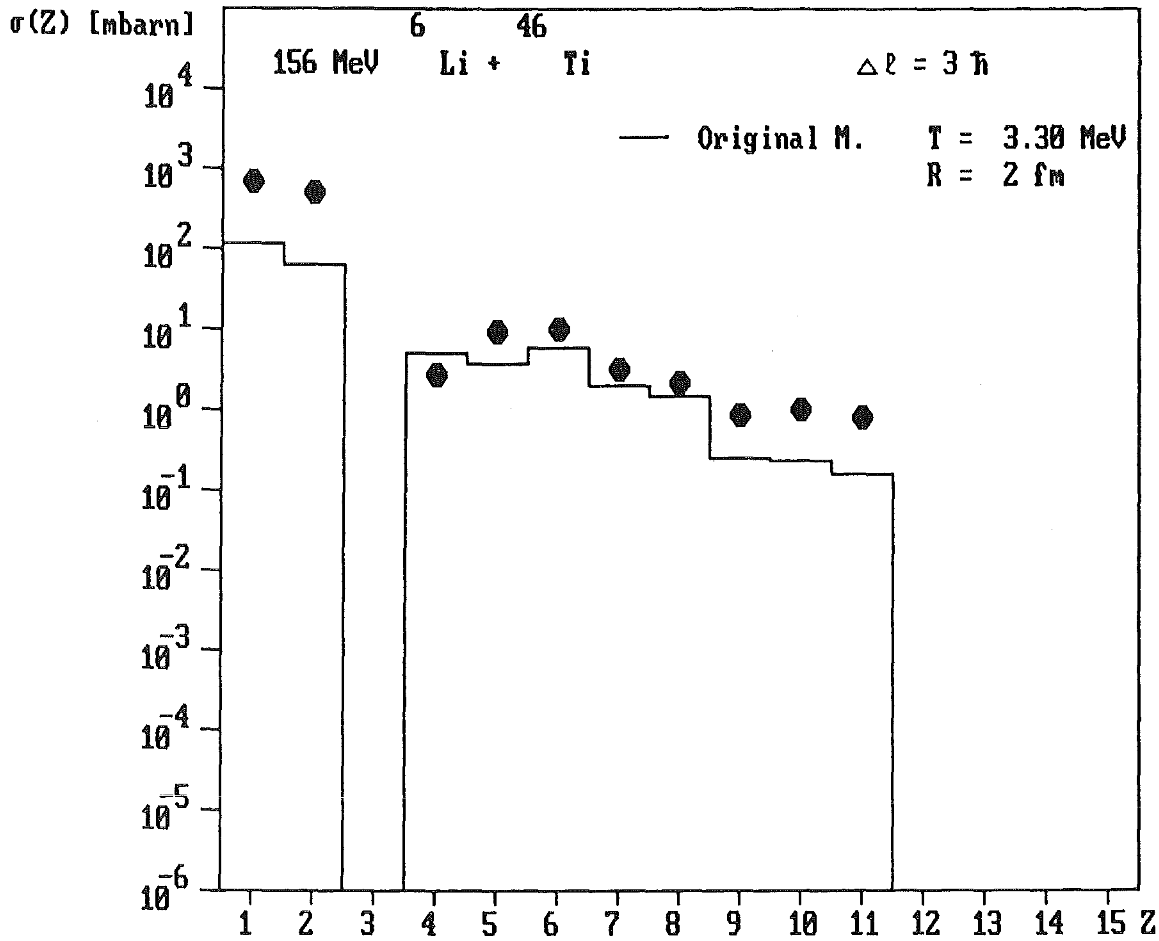

Fig. 12 Results of the analysis of IMF emission from collisions of 156 MeV ^{6}Li ions with ^{46}Ti: experimental results /16/ compared with predictions of the *original* sum-rule model.

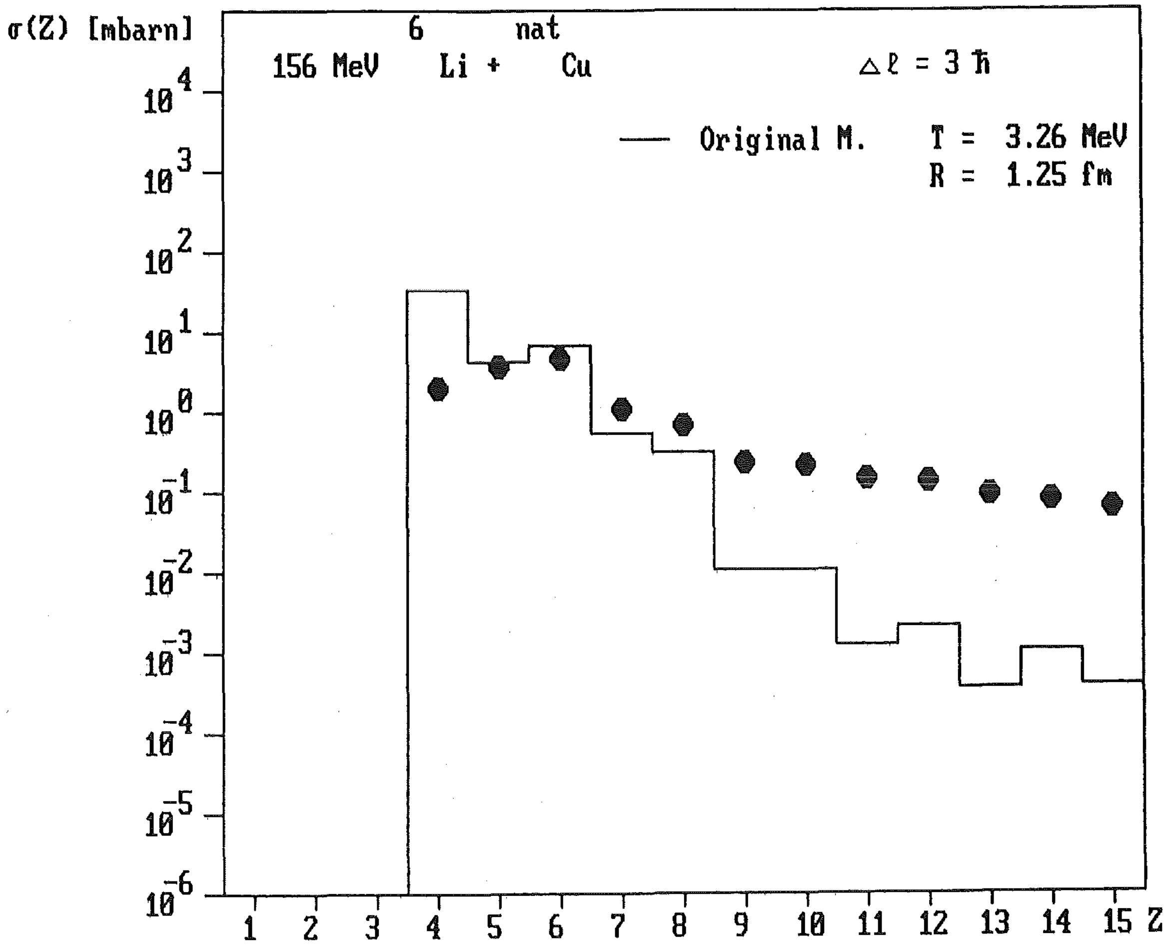

Fig. 13 Results of the analysis of IMF emission from collisions of 156 MeV ^{6}Li ions with ^{nat}Cu: experimental results /17/ compared with predictions of the *original* sum-rule model.

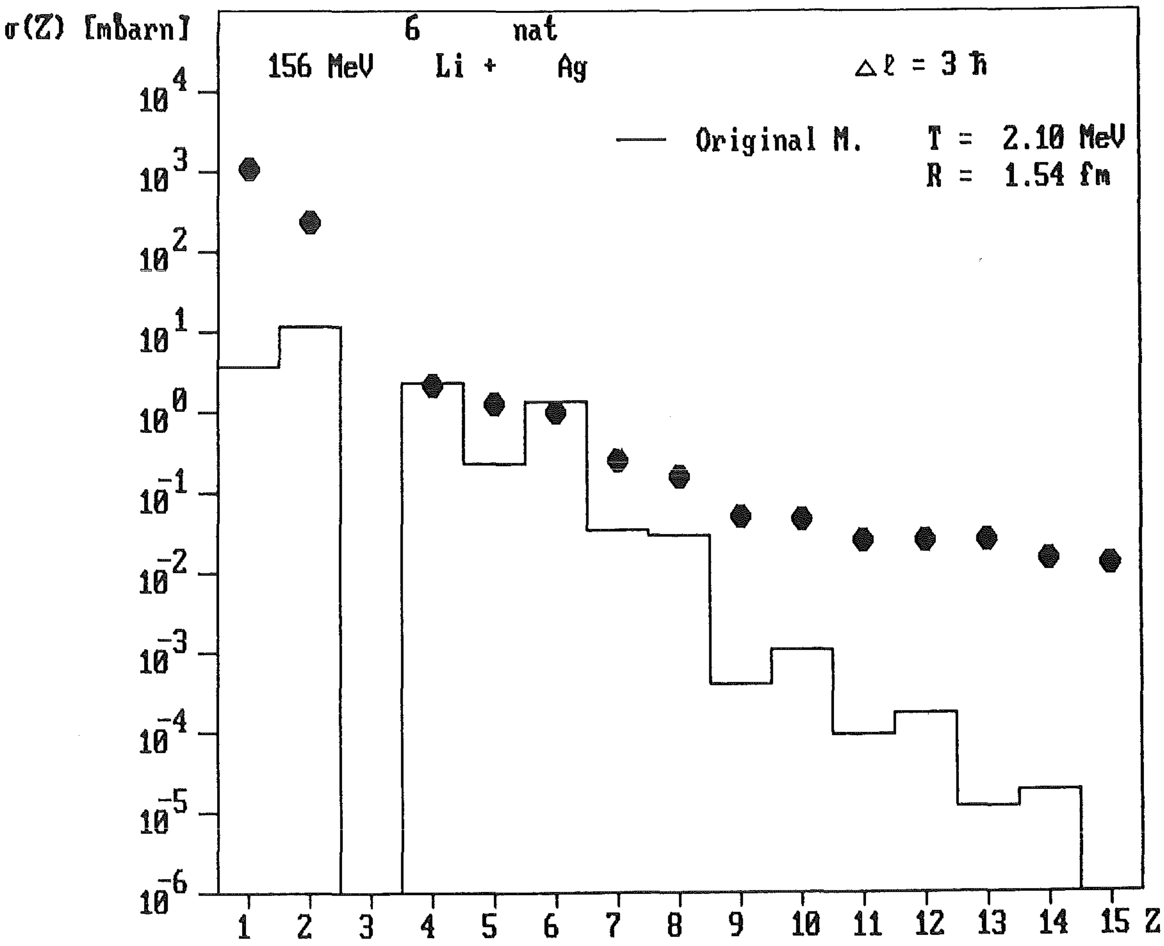

Fig. 14 Results of the analysis of IMF emission from collisions of 156 MeV ^{6}Li ions with ^{nat}Ag: experimental results /17, 18/ compared with predictions of the *original* sum-rule model.

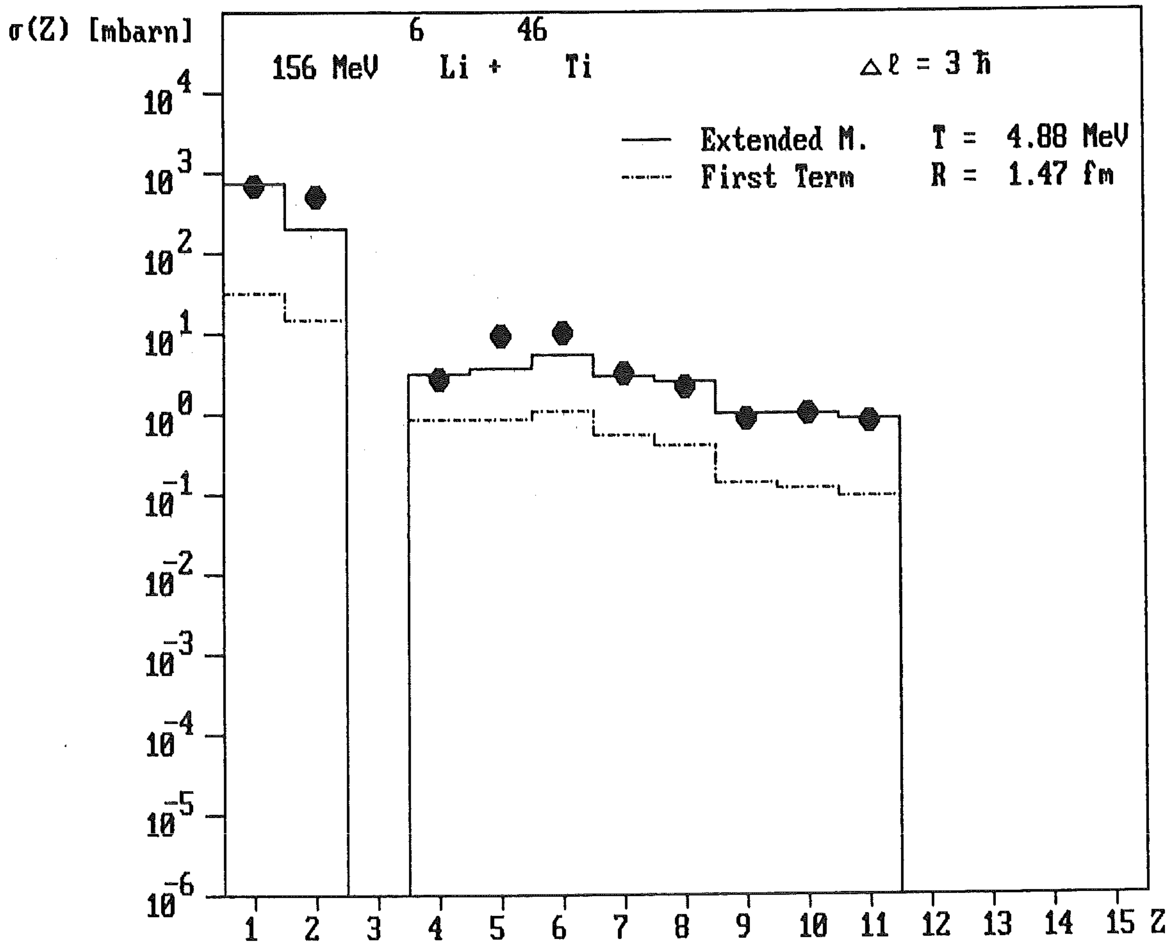

Fig. 15 Results of the analysis of IMF emission from collisions of 156 MeV ^{6}Li ions with ^{46}Ti /16/ based on the *extended* sum-rule. The dashed curve represents the contribution of the original model.

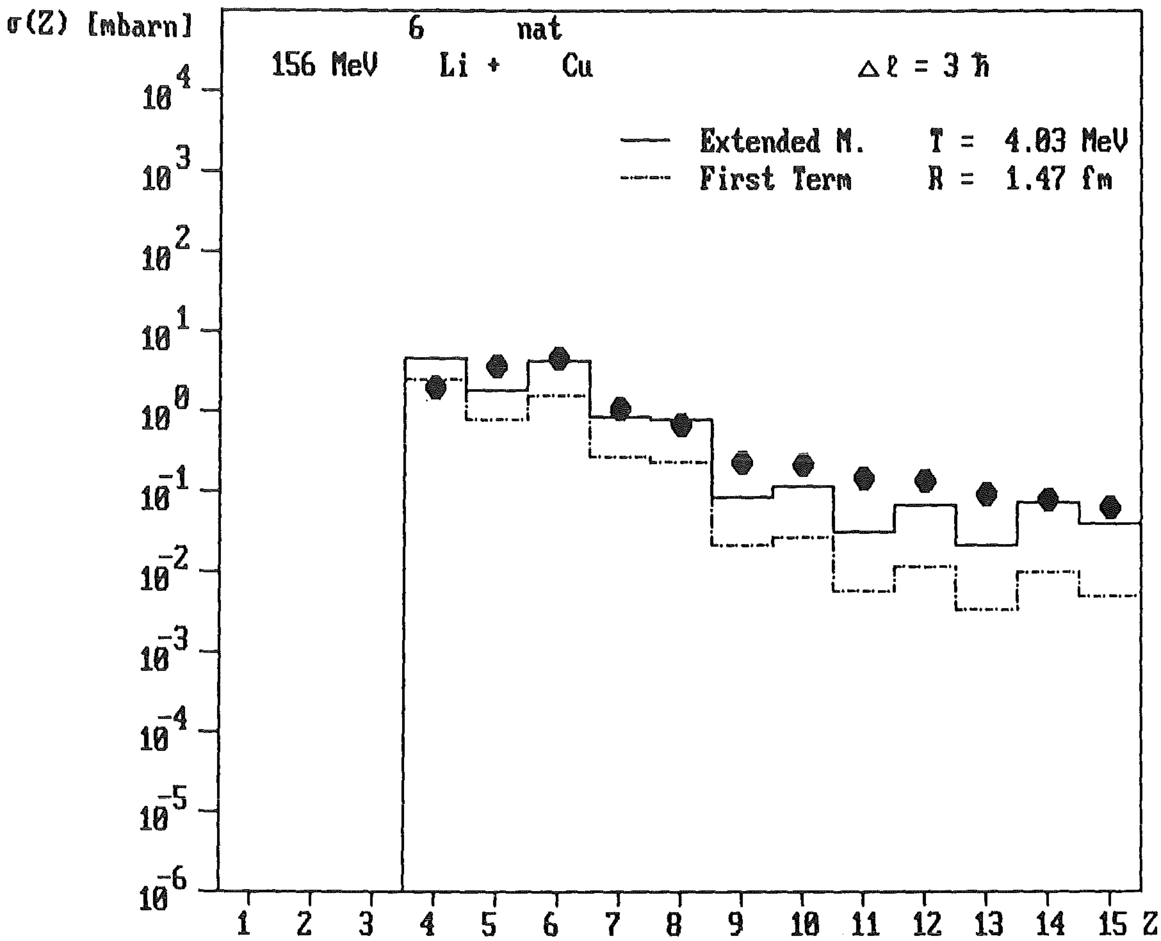

Fig. 16 Results of the analysis of IMF emission from collisions of 156 MeV ^{6}Li ions with ^{nat}Cu /17/ based on the *extended* sum-rule. The dashed curve represents the contribution of the original model.

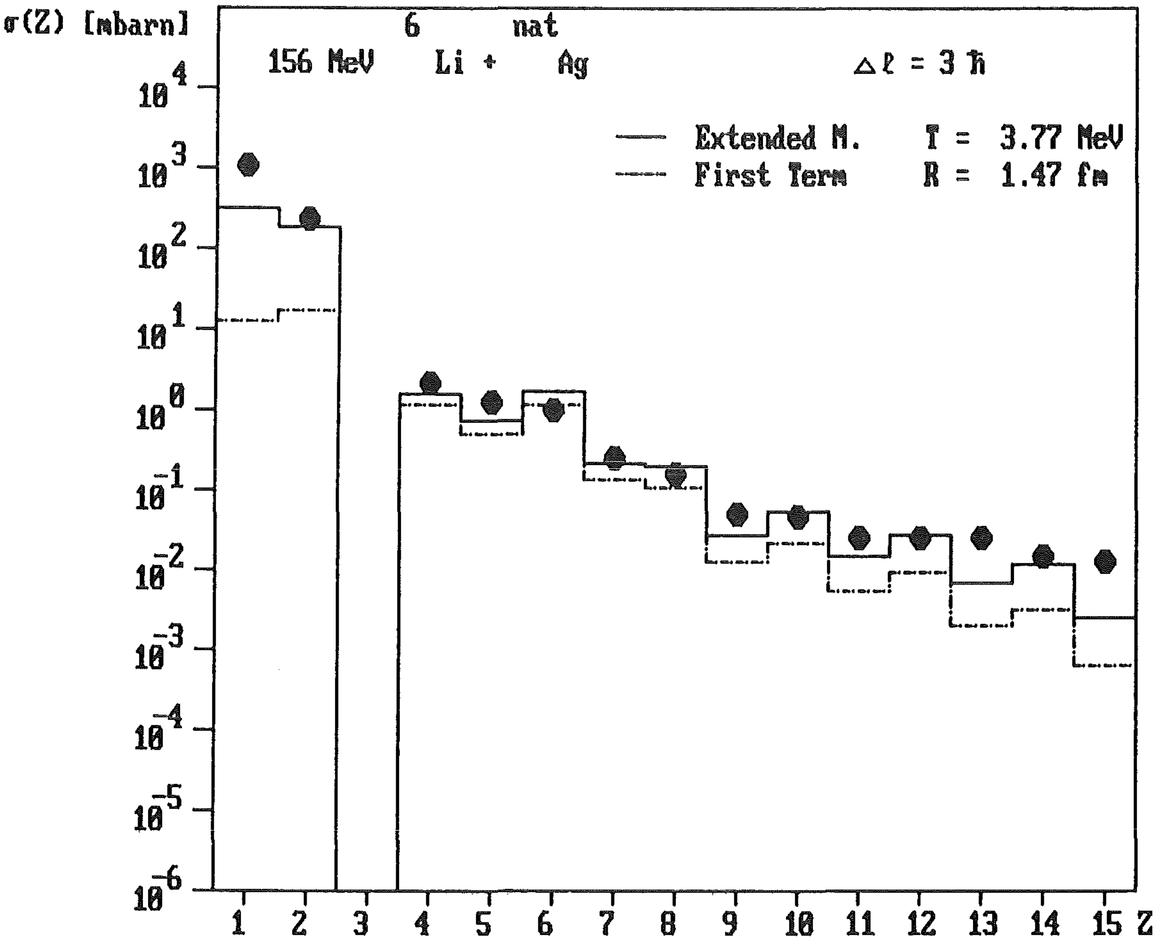

Fig. 17 Results of the analysis of IMF emission from collisions of 156 MeV ^{6}Li ions with ^{nat}Ag /17, 19/ based on the *extended* sum-rule. The dashed curve represents the contribution of the original model.

8. Conclusions

Assuming that the IMF emission originates from a partial statistical equilibrated process, an extended sum-rule model is proposed for the calculation of the reaction cross sections. For each partial wave ℓ, a term, additional to the original sum-rule /4, 5/, is included which takes into account the emission of light products from a transient dinuclear system on its route to complete fusion. Thus, the reaction cross section for each exit channel (i) is a sum of two contributions, $\sigma(i)$, representing the incomplete fusion and $\sigma'(i)$, responsible for the emission from the dinuclear system.

Recent results /20/ about ^{40}Ar induced reactions with Ag at E/amu = 27 MeV support the idea of the extension of the sum-rule model. They indicate that the major fraction of the IMF emerges from deeply inelastic collisions.

In the considered cases of reactions of 336 MeV ^{40}Ar with heavy targets, the emission of $3 \leqq Z \leqq 9$ products at large angles is well reproduced by the new term $\sigma'(i)$. The IMF emission in the ^{6}Li + ^{46}Ti, ^{nat}Cu and ^{nat}Ag reactions at 156 MeV is remarkable well predicted by the extended sum-rule model. Such asymmetric cases prove to be a rather good experimental basis for explaining the features of the model.

Acknowledgement

I would like to express my gratitude to Prof. Dr. M. Petrascu for his permanent interest in this work and his guiding advice. The pleasant and inspiring collaboration with Dr. Anisoara Constantinescu is well appreciated. The encouragement and valuable comments of Prof. Dr. M. Ivascu whose help enabled the progress of this work in many aspects, is gratefully acknowledged.

This report and a part of the calculations were done during a research visit in Kernforschungszentrum Karlsruhe. I would like to thank the International Bureau of Kernforschungszentrum Karlsruhe and the Institut für Kernphysik for the kind hospitality during my visit, in particular to Prof. Dr. G. Schatz and Prof. Dr. H. Rebel, also for clarifying discussions, encouragement and substantial help. I acknowledge helpful comments of Dr. D. K. Srivastava, and the support of Dipl. math. J. Oehlschläger and J. Wentz in managing computer problems. Last not least, I would like to thank for stimulating discussions with Prof. Dr. V. Volkov whose work did the impact to the present studies and with Dr. C. Ngô who supplied me also with the computer program "SURPLUS".

References

1. J.P. Bondorf, F. Dickmann, D.H.E. Gross and P.J. Siemens, Journ. de Phyique, Colloq. (1971) No. 6, 145
2. J. Wilczyński, Nucl. Phys. A216 (1973) 386
3. K.Siwek-Wilczyńska E.H. du Marchi van Voorthuysen, J. van Popta, R.H. Siemssen and J. Wilczyński, Phys. Rev. Lett. 42 (1979) 1599
4. J. Wilczyński, K. Siwek-Wilczyńska, J. van Driel, S. Gonggrijp, D.C.M. Hageman, R.V.F.Janssens, J. Lukasiak and R.M. Siemssen, Phys. Rev. Lett. 45 (1980) 606
5. J. Wilczyński,.K. Siwek-Wilczyńska, J. van Driel, S. Gonggrijp, D.C.M. Hageman, R.V.F.Janssens, J. Lukasiak, R.M. Siemssen and S.Y. van der Werf, Nucl. Phys. A373 (1982) 109
6. V.V. Volkov, contributed papers to 2nd Internat. Conf. on Nucleus-Nucleus Collisions, Visby, Sweden, June 10-14, 1985, C. 18, 19
7. A.G. Artukh, V.V. Avdeichikov, J. Erö, G.F. Gridnev, V.L. Mikheev, V.V. Volkov and J. Wilczyński, Nucl. Phys. A160 (1971) 511
8. C. Ngô, Progr. Part Nucl. Phys., Vol. 16, p. 139, Pergamon Press 1986
9. C. Ngô, Proc. Int. School on critical phenomena in heavy ion physics, Poiana Brasov (1980), Romania p. 395, and private communications
10. C. Ngô, B. Tamain, M. Beiner,.R.J. Lombard, D. Mas and H.H. Deubler, Nucl. Phys. A252 (1975) 237
11 D.H.E. Gross, Lect. Notes in Physics., Vol. 33, p. 194 Springer Berlin, 1974
12 I.M. Brâncuş, I. Berceanu, A. Buţă, C. Grama, I. Lazăr, I. Mihai, M. Petraşcu, V. Simion and A. Constantinescu, Z. Phys. A320 (1985) 443
13. T. Suomijarvi, R. Lucas, C. Ngô, T. Tomasi, D. Dalili and T. Matuszcek, Nuovo C 82A (1984) 51
14. L.C. Vaz, D. Logan, J.M. Alexander, E. Dudek, D. Guerreau, L. Kowalski, M.F. Rivet and M.S. Zisnan, Z. Phys. A311 (1983) 89
15. M. Petraşcu, I.M. Brâncuş, A. Buţă, I. Mihai, V. Simion, V.V. Volkov, A.G. Artukh and A.N. Mesentsev, Rev. Roum. Phys. 33 (1988) 795
16. T. Kozik, H. Buschmann, K. Grotowski, H.J. Gils, N. Heide, J. Kiener, H. Klewe-Nebenius, H. Rebel, S. Zagromski, A.J. Cole and S. Micek, Z. Phys. A326 (1987) 421

17 K. Grotowski, J. Ilnicki, T. Kozik, J. Lukasik, S. Micek, Z. Sosin, A. Wieloch, N. Heide, H. Jelitto, J. Kiener, H. Rebel, S. Zagromski and A.J. Cole, Phys. Lett. B (submitted)
T. Kozik et al., Internal Report of Kernforschungszentrum Karlsruhe, Dez. 1987

18 I.M. Brâncuş, J. Oehlschläger and J. Wentz, KfK-Report 4454 B (1988)

19 J. Wentz, N. Heide, V. Corcalciuc, S. Zagromski, H. Rebel, I.M. Brâncuş, (in preparation)

20 B. Borderie, M. Montoya, M.F. Rivet, D. Jouan, C. Cabot, H. Fuchs, D. Gardes, H. Gauvin, D. Jacquet and F. Monet, Phys. Lett. B205 (1988) 26